Structural Analysis of G-DNA in Solution: A Combination of Polarized and Depolarized Dynamic Light Scattering with Hydrodynamic Model Calculations†

M. Bolten, M. Niermann, and W. Eimer*

Physikalische Chemie I, Universität Bielefeld, Universitätsstrasse 25, 33625 Bielefeld, FRG

Received March 31, 1999; Revised Manuscript Received June 15, 1999

ABSTRACT: Specific intra- and intermolecular quadruplex conformations of model G-DNA oligonucleotides have been identified from their translational and rotational diffusion coefficients in aqueous solution. The transport properties were determined by polarized and depolarized dynamic light scattering. A comparison with hydrodynamic model calculations provides detailed information about the size and shape of the molecules and allows one to distinguish between alternative intra- and intermolecular association. The potential of this combination of methods to elucidate biomolecular structures in solution, to characterize conformational changes, and follow intermolecular interaction processes due to a response to external stimuli has been discussed.

Oligonucleotides that contain single or multiple guanine-rich segments are known to form specific four-stranded helical conformations in solution. This novel structural motif was first related to the highly repetitive ends of chromosomes, known as telomeric DNA (*1*, *2*), but was found later in other naturally occurring stretches of DNA and RNA (*2*). The formation and stability of these novel DNA conformations are strongly dependent on the presence of monovalent cations with an extraordinary selectivity for potassium (*3*, *4*). Moreover, single strands with multiple guanine regions can form intra- and/or intermolecular associates. It is well-conceivable that this polymorphism together with the cation specificity plays an important role in recognition and regulation processes in biological systems. To understand the switching mechanism between polymorphous structures, it is essential to obtain detailed information about the structure and equilibrium properties of quadruplex forming oligonucleotides under different environmental conditions (kind of cation, ionic strength, etc.) in solution.

The formation and specific conformational characteristics of G-DNA have been investigated by X-ray crystallography (*5*), NMR-spectroscopy (*6*) as well as by chemical probing and other spectroscopic techniques (*7*). First evidence for the existence of a quadruplex conformation came from X-ray crystallography on poly-G helices (*8*). The formation of four-stranded helical structures has been confirmed for short model oligonucleotides in solution and in crystalline state (*5*, *6*). As shown in Figure 1a, the basic structural motive of these sequences is the G-quartet that consists of four guanine bases in a square planar array, which are stabilized by a cyclic hydrogen-bonding pattern, where each guanine is both the donor and acceptor of two hydrogen bonds (*4*). The center of the G-quartet is lined by four electronegative carbonyl oxygens. This pocket is large enough to act as a coordination site for cations. The specific cation complexation together with the strong hydrogen-bonding interaction explain the stability of the tetrameric arrangement. In G-DNA, mostly two to four of these guanine quartets are stacked to form helical quadruplex structures. The stacking of individual G-quartets results in the formation of a channel that creates another specific interaction site for cations, now between two

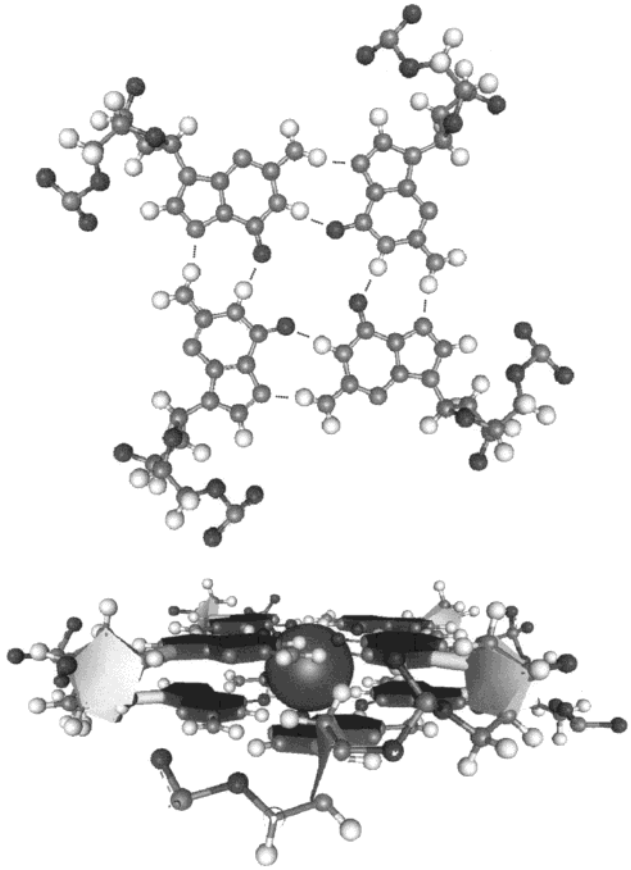

FIGURE 1: (a) Molecular representation of a G-quartet; (b) molecular representation of two stacked G-quartets. The carbonyl O6-oxygen atoms of the guanine bases form a twisted cage with a potassium cation inside.

† This work was supported by a grant from the Deutsche Forschungsgemeinschaft (Ei 221/5-2).

* To whom correspondence should be addressed. E-mail: weimer@pc1.chemie.uni.bielefeld.de.

10.1021/bi990750p CCC: $18.00
Published on Web 08/26/1999

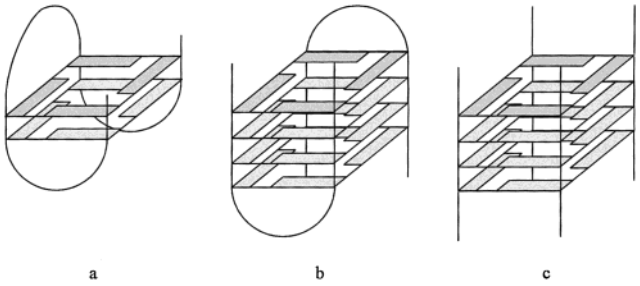

FIGURE 2: Schematic representation of quadruplex structures with different strand stoichiometries. (a) monomer intramolecular quadruplex; (b) dimer inter/intramolecular quadruplex through association of two "hairpin" strands; (c) tetramer intermolecular quadruplex through association of four single strands.

G-quartets, where the eight carbonyl O6-oxygen atoms of the guanine bases form a twisted cage (see Figure 1b).

It is known that the formation of tetraplex structures through intra- or intermolecular association depends on the DNA-concentration and the given temperature (*4*, *9*). But one of the most fascinating aspects of G-rich DNA is its highly specific interaction with mono- and divalent cations (*7*). A number of structural and thermodynamic studies on different G-DNA molecules reveal that cations induce and stabilize quadruplex formation in the order $K^+ > Na^+ > Li^+ > Rb^+ > Cs^+$ for monovalent ions, and $K^+ > Ca^{2+} > Mg^{2+}$ for divalent cations. Some exceptions from this general sequence have been found (*10*, *11*). With an increasing number of G-segments, different polymorphous arrangements from intra- or intermolecular association can occur (see Figure 2). These conformations differ in strand stoichiometry, G-quartet and loop geometry, or in the local conformation of the sugar residues.

To understand the biological role and to predict medical and technical applications of G-DNA, it is important to study these systems under a wide variety of environmental conditions (temperature, salt concentration, etc.) in solution. For this purpose, dynamic light scattering (DLS)[1] is a very powerful noninvasive tool which allows one to investigate the dynamics of macromolecular systems (*12*). Although, DLS does not approach the resolution power of X-ray crystallography or NMR spectroscopy, it provides valuable complementary information about translational and rotational motion of particles in solution. These transport properties are highly sensitive to the size and shape of molecules and, of course, to intermolecular interactions that lead to association or ordered structures (*9*). Hence, the overall molecular dimensions of biomolecules as well as conformational changes of proteins and DNA have been characterized by light scattering techniques (*11*, *13*). The interpretation of experimental results from DLS can be substantially refined in combination with hydrodynamic model calculations, which provide predictions for the transport coefficients based on detailed model structures (*14*, *15*).

We have applied these experimental and theoretical methods to investigate the specific conformational variability of model oligonucleotides under physiological conditions. The measurements have been performed over a wide range of temperature and salt concentration. The primary aim of this work was to test the potential of these complementary methods to characterize hydrodynamic properties, and hence, to identify and differentiate between alternative DNA quadruplex conformations in solution. For this reason, we have selected three G-DNA model sequences where, as reference points, the conformation is known from X-ray crystallography or from NMR spectroscopy for given environmental conditions in solution.

[1] Abbreviations: NMR, nuclear magnetic resonance; poly-G, poly guanylic acid; DLS, dynamic lights scattering; Tris, 2-amino-2-(hydroxymethyl)-1,3-propanediol; EDTA, ethylene diamine tetra acetic acid; SE, Stokes-Einstein; SED, Stokes-Einstein-Debye; 5′-GMP, 5′-guanosine monophosphate; PAGE, polyacrylamide gel electrophoreses.

MATERIAL AND METHODS

Materials. The oligonucleotides $d[G_2T_2G_2T]_2G$ (15-mer) and $d[T_2G_4T_2]$ (8-mer) were purchased in lyophilized form from OSWELL, and the 14-mer $d[T_2G_4T]_2$ was obtained from MIDLAND. All samples were delivered free of salt and with a purity higher than 98%.

For the dynamic light scattering measurements, the material was dissolved in TE-buffer (10 mM Tris, 0.1 mM EDTA, pH 7.1). The final potassium concentration was adjusted by adding a concentrated aqueous solution of KCl. Every solution was filtered through Anotop 10 (plus) 0.02 μm filters. After filtration, the oligonucleotide concentration was controlled by UV−vis spectroscopy. (μmolar extinction coefficient (μM^{-1} cm^{-1}) at 260 nm: 73.8 $d[T_2G_4T_2]$, 142.3 $d[G_2T_2G_2T]_2G$, and 131.8 $d[T_2G_4T]_2$).

Depolarized Dynamic Light Scattering. The depolarized component of scattered light was measured in a standard depolarized dynamic light scattering experiment, which has been described in detail in (*12*, *16*). The light source was a solid-state Nd:YAG laser (Coherent, Model DPSS-400) operating in single mode at $\lambda = 532$ nm. The light scattered at 90° in the VH geometry (vertical polarization of the incident beam and horizontal polarization of the scattered beam) was frequency analyzed by a piezo-driven Fabry−Perot interferometer equipped with a set of confocal mirrors with a free spectral range of 0.75 and 2 GHz, respectively. This setup allows the analysis of slow relaxation processes on the order of nanoseconds. The detection system consists of an Hamamatsu photomultiplier tube (Model R464), an ORTEG amplifier discriminator, and a WindowsPC based data acquisition unit (ISA-MCSII multichannel scaler card, OXFORD Instruments). A reference beam of unscattered light was used to monitor the instrumental line width at the beginning and end of each interferometer scan. All data were deconvoluted by an iterative method (*16*, *17*). The rotational relaxation time was calculated form the half-width at half-height, Γ, of the spectra, fitted to a Lorentzian with

$$\tau_r = \frac{1}{2\pi\,\Gamma_r} \tag{1}$$

The correlation time, τ_r, is related to the rotation diffusion coefficients and hence to the hydrodynamic radius of the molecules according to

$$D_r = \frac{1}{6\tau_r} \tag{2}$$

and

$$R = \left(\frac{kT}{8\pi\eta_0 D_r}\right)^{1/3} \quad (3)$$

Polarized Dynamic Light Scattering. Translation diffusion coefficients were measured by photon correlation spectroscopy (*9*, *18*, *19*). The light source was an argon ion laser (Coherent, model INNOVA-90) operated with an output power between 200 and 600mW at $\lambda = 488$ nm. The vertically polarized component of scattered light was analyzed by an ALV-5000 digital correlator with a fast card extension. Translation diffusion coefficients were obtained using the standard data analysis program CONTIN (20). The normalized field autocorrelation function is presented by

$$g_1(\tau_t) = \int_0^\infty G(\Gamma_t) \exp(-\Gamma_t \tau_t) d\Gamma_t$$

where $G(\Gamma_t)$ is a distribution function of relaxation processes which is proportional to the *z*-averaged size distribution of the scattering molecules. The average value of Γ_t is related to the translational diffusion coefficients D_t according to

$$\bar{\Gamma}_t = D_t q^2 \quad (4)$$

where q is the absolute value of the scattering vector ($q = 4\pi n/\lambda \sin(\theta/2)$), with n the refractive index of the solution, λ the wavelength of scattered light, and θ the scattering angle. From the translational diffusion coefficient D_t, the hydrodynamic radius is calculated using the Stokes−Einstein equation

$$D_t = \frac{kT}{6\pi\eta_0 R_h} \quad (5)$$

Hydrodynamic Model Calculations. The hydrodynamic properties, namely, the rotational and translational diffusion coefficients for the oligonucleotides of different conformation, were calculated using the "bead" model for rigid macromolecules (*16*, *21*). The concept behind this theoretical model is that the detailed molecular structure of DNA-conformers (or any rigid macromolecule) can be modeled by an assembly of spherical subunits. These frictional elements may either represent individual atoms, specific molecular residues (e.g., the sugar moiety, the nucleobases, etc.) or arbitrary subunits, depending on the level of refinement.

Each of these beads are considered as a source of local friction assigned with a frictional coefficient according to Stokes law

$$\zeta_i = 6\pi\eta_0 r_i \qquad \text{for translation}$$

$$\zeta_i = 8\pi\eta_0 r_i^3 \qquad \text{and for rotation}$$

where η_0 is the solvent viscosity and r_i an effective radius of the corresponding i-th spherical element.

We have developed a computer program to calculate the rotational and translational diffusion coefficients for different DNA conformers (*16*, *22*). In general, this program is based on the bead model procedure by Bloomfield and Garcia de la Torre (*23*). The molecular input structures for the hydrodynamic calculations were obtained using the program HYPERCHEM (*24*) or from crystallographic data from the Brookhaven data bank (*25*). Moreover, we have developed a computer program to generate arbitrary four-stranded quadruplex structures from planar tetrameric units. Through the use of HYPERCHEM, sodium ions were placed in a distance of 1.688 Å to each phosphate group of the backbone to neutralized the negative charges.

Each oligonucleotide was placed into a water bath (SPC/E) (*26*). Thereafter, each system was equilibrated using the GROMOS87 molecular mechanics force field (*26*). The final thickness of the hydration shell was chosen according to geometric considerations. To account for the limited access of inner frictional elements to the solvent, an effective hydrodynamic radius for each sphere was calculated that was dependent on the accessible surface area of each individual bead to the solvent. We have used the model by Lee and Richards (*27*) to determine the solvent accessible surface area (ASA), which is obtained by rolling a probe sphere over the surface of the macromolecule, where the finite probe size can be chosen in such a way to reflect the molecular dimensions of the solvent molecules (e.g., 1.4 Å for water). Details of the hydrodynamic model calculations can be found in ref (*16*, *22*).

RESULTS AND DISCUSSION

We have investigated the potential of dynamic light scattering techniques in combination with hydrodynamic model calculations to distinguish between different DNA conformations in solution. Three different oligonucleotides were chosen as model compounds for polymorphous conformations of G-DNA.

(1) The 15-mer d[GGTTGGTGTGGTTGG], a 15 base long DNA fragment known as thrombin binding aptamer, has been characterized by X-ray crystallography and NMR spectroscopy (*28*, *29*). In the crystalline state as well as in solution in the presence of KCl, the experimental results indicate that the molecule forms an intramolecular quadruplex structure of almost spherical shape (Figure 2a).

(2) A 14-mer d[TTGGGGTTGGGGTT] where NMR data obtained from a 12-mer d[GGGGTTTTGGGG] (*30*) with an analogous sequence is comprised of a G stem and a T loop region, which provides evidence for a dimer inter/intramolecular quadruplex structure through association of two "hairpin" molecules (Figure 2b).

(3) An 8-mer d[TTGGGGTT], with a single guanine-rich region, where homologous oligonucleotides (which differ in the number of thymine residues) are known to exist as intermolecular G-quartets in the presence of potassium (*5*, *31*) (Figure 2c).

The rotational motion of these oligonucleotides has been investigated by depolarized dynamic light scattering in aqueous solution in the presence of potassium ions. The temperature-dependence of the rotational correlation times is presented in a Stokes−Einstein−Debye (SED) plot according to

$$\tau_r = \frac{1}{6D_r} = \frac{V_h}{k} \times \frac{\eta_0}{T} + \tau_0 \quad (6)$$

where D_r is the rotation diffusion coefficient, V_h is the effective hydrodynamic volume, and η_0 the viscosity of the solvent. τ_0 has been included in this empirical equation to

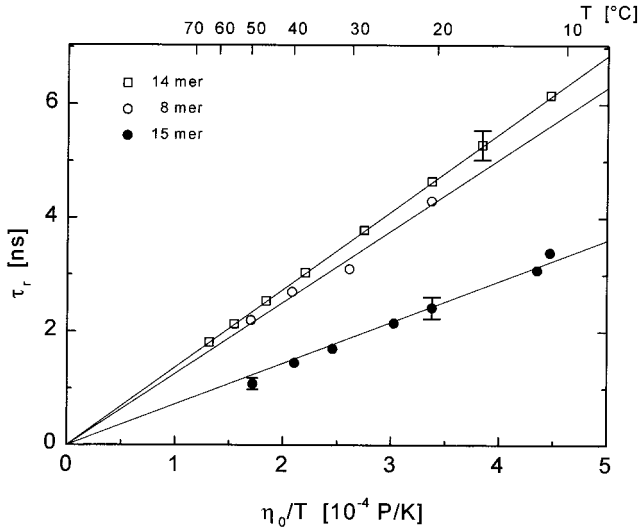

FIGURE 3: Stokes−Einstein−Debye plot of the rotational relaxation times for various quadruplex structures. (□) 14-mer d[TTGGGGTTGGGGTT]$_2$; 1.38 mM in 45 mM KCl forming an intermolecular quadruplex (see Figure 2b); (○) 8-mer d[TTGGGGTT]$_4$; 3.12 mM in 48 mM NaCl as an intermolecular quadruplex (Figure 2c); (●) 15-mer d[GGTTGGTGTGGTTGG]; 1.48 mM in 53 mM KCl forming a monomer intramolecular quadruplex (Figure 2a).

Table 1: Hydrodynamic Properties of the Model Quadruplex Oligonucleotides

oligonucleotide	τ_r^{20} [ns]	D_t^{20} [10^{-6} cm^2/s]	V_h [nm^3]
14-mer	4.71	1.48	19.03
8-mer	4.3	1.34	17.37
15-mer	2.48	1.8	10.02

take into account a nonzero intercept sometimes observed in experimental studies (*32*).

First of all, for all three model compounds, we observed a linear dependence of τ_r on η_0/T with a zero intercept (Figure 3), indicating that the SED equation does represent the experimental data. Although the 15-mer d[GGTTGGTGTGGTTGG] and the 14-mer d[TTGGGGTTGGGGTT] differ in length only by one nucleobase, they exhibit significantly different relaxation times, with the longer oligonucleotide being much faster. This finding indicates that the two compounds arrange in different conformations in solution under similar conditions. The significantly shorter relaxation time of the 15-mer suggests that it exists in a more compact form than the 14-mer. For the 8-mer d[TTGGGGTT], we measured almost the same relaxation times as for the much longer 14-mer, which led us to assume that the molecules associate to higher ordered structures in the presence of KCl. An overview of the hydrodynamic properties is given in Table 1.

To further elucidate this conformational diversity of the model oligonucleotides, we will compare the dynamic light scattering results with experimentally determined diffusion coefficients from oligonucleotides of known structure in solution as well as with hydrodynamic model calculations.

15-mer d[GGTTGGTGTGGTTGG]. In the presence of potassium ions, the 15-mer exhibits an unusually short rotational relaxation time, considering its length. Complementary, we have determined the translational diffusion coefficient by photon-correlation spectroscopy. Results from the temperature-dependent measurements are displayed in

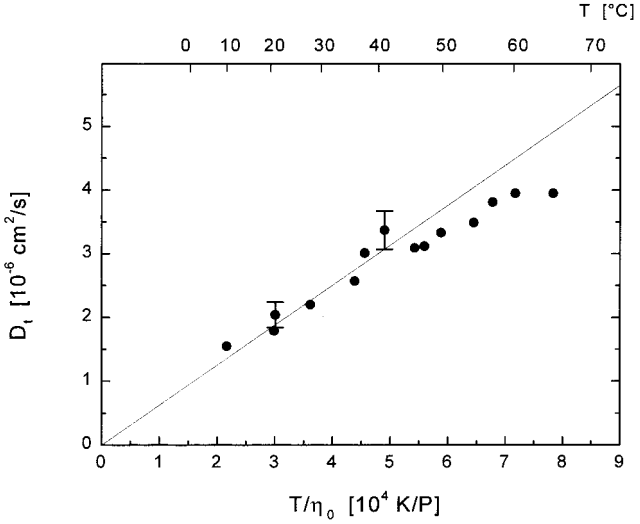

FIGURE 4: Temperature dependence of the translational diffusion coefficient of the aptamer d[GGTTGGTGTGGTTGG] (●). The concentration of the oligonucleotide is 1.48 mM in 53 mM KCl.

Figure 4. According to the Stokes−Einstein equation (eq 5), we observed a linear-dependence of the diffusion coefficient D_t on T/η_0 up to 45 °C. At higher temperatures, however, the translational diffusion coefficient is significantly smaller than expected from the Stokes−Einstein behavior at low temperature. For $T > 45$ °C, the nonlinear behavior of D_t with T/η_0 indicates that the hydrodynamic volume increases with temperature, suggesting that a conformational change occurs.

To obtain detailed information about the size and shape of the oligonucleotide under the given solution conditions, we have calculated the translational diffusion coefficients and rotational relaxation times from hydrodynamic theory. A comparison of model predictions and experimental data for different DNA conformations of similar length, with our depolarized dynamic light scattering results, is presented in Figure 5 and Table 2. The rotational correlation times as well as the measured translational diffusion coefficients of the 15-mer are in best agreement with model predictions for an intramolecular tetraplex conformation (see schematic representation in Figure 2a). It becomes quite obvious from Figure 5 that the formation of double-helical or "hairpin" structures can be safely excluded in aqueous solution in the presence of 53 mM KCl.

The nucleotide sequence of the 15-mer d[GGTTGGTGTGGTTGG] is not self-complementary in any part of the molecule, and hence, the oligonucleotide cannot form the typical Watson−Crick double-helical structure as well as it is highly unlikely to exist in a "hairpin" conformation. Nevertheless, to demonstrate the potential of the dynamic light scattering techniques for a conformational analysis in solution in general, we have compared the rotational relaxation times of the 15-mer with a 17 bases long oligonucleotide d[(CG)$_3$TTGTT(CG)$_3$] in a "hairpin" conformation and a 16-bp duplex d[(AT)$_3$(CG)$_2$(AT)$_3$] (see Figure 5). Furthermore, we have calculated the rotational correlation time for an extended single-stranded structure of the same length as the 15-mer. It becomes clearly evident that the relaxation behavior of the various conformational structures is significantly different and easily distinguishable by de-

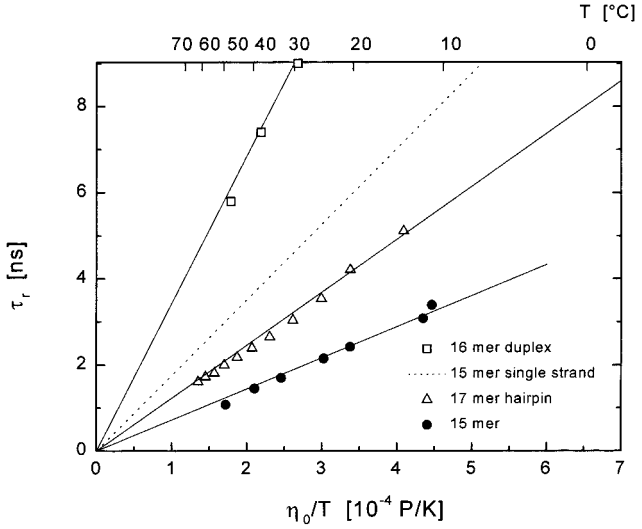

FIGURE 5: Temperature dependence of the rotational correlation times of the (●) 15-mer d[GGTTGGTGTGGTTGG]; 1.48 mM in 53 mM KCl. Comparison with experimentel data for a 17 nucleobases long "hairpin" conformation (△) d[$(CG)_3$TTGTT$(CG)_3$] (from ref 35); 1.7 mM in 100 mM NaCl. The full lines correspond to a linear regression of the experimental data. Hydrodynamic model calculations for a single-strand (···) structure with a length of 15 nucleobases and a 16 bp Watson−Crick duplex (identical with experimental data (□) from ref 19).

polarized dynamic light scattering. Because of the $1/R^3$ dependence of the rotational diffusion coefficient (see eq 3), depolarized dynamic light scattering is superior to other methods that measure the translational diffusion coefficient where $D_t \sim 1/R$ (SE-equation; eq 5).

In summary, considering the base sequence of the oligonucleotide, the 15-mer d[GGTTGGTGTGGTTGG] could exist in an elongated or refolded (quadruplex) single-stranded conformation in solution. The data in Figure 5 and Table 2 strongly support the existence of an intramolecular quadruplex conformation in the presence of KCl.

8-mer d[TTGGGGTT]. The temperature-dependence of the rotational and translational motion of the 8-mer is displayed in Figure 6. The oligonucleotide consists of a single guanine-rich region, and hence, can form a G-DNA conformation only through association of four individual strands in solution (Figure 2c). Further longitudinal aggregation is prevented by the two thymine bases at both ends of the model compound. As shown in Figure 6 and Table 3, the experimental data are in excellent agreement with hydrodynamic model calculations for an intermolecular tetraplex conformation. From NMR measurements, the existence of a considerable amount of individual single-stranded structures at room temperature can be safely excluded under the given salt concentration (*31*).

In the polarized dynamic light scattering measurements beyond $T \approx 55$ °C, however, we observed a significantly larger translational diffusion coefficient than expected from the low-temperature data. The deviation from the Stokes−Einstein behavior indicates a decrease in the hydrodynamic volume that can be attributed to a melting and breaking up of the quadruplex structure at high temperature. Similar results have been obtained by dynamic light scattering experiments where Eimer and Dorfmüller observed the melting of tetraplex structures of 5′-GMP (*9*). Henderson et al. performed temperature-dependent PAGE, detecting an unfolding of $d[TTGGGG]_4$ at 55 °C [**1**], while Balagurumoorthy et al. also reported a melting of tetraplex structures from $d[G_4T_{(2-4)}G_4]$ (in 70 mM NaCl) studies by CD and molecular migration in nondenaturing gel electrophoresis (*33*).

14-mer d[TTGGGGTTGGGGTT]. This 14 base long oligonucleotide contains two guanine-rich regions, which enables the formation of a four-stranded intermolecular tetraplex structure as well as a "hairpin" G-DNA conformation through association of two refolded strands as displayed in Figure 2b. The temperature-dependence of the transport properties of the model compound from polarized and depolarized dynamic light scattering experiments are displayed in Figures 7 and 8.

As observed for the other oligonucleotides studied, the rotational correlation times follow the Stokes−Einstein−Debye equation within the temperature range 8 °C ≤ T ≤ 66 °C. Measurements have been performed for three different DNA concentrations and in the presence of 16 and 45 mM KCl, respectively. All data are represented by a single master curve, indicating that within the experimental error no concentration effects can be detected. The correlation times are significantly slower than measured for a 13 base pair fragment that is known to form an intramolecular "hairpin" structure (*14*, *34*). On the other hand, we have calculated the transport coefficient for a G-DNA quadruplex, comprising of four individual strands with a length of 14 bases. For this model structure the predicted rotational relaxation times are much longer than experimentally observed for the 14-mer. Hence, the existence of both conformations can be excluded in aqueous solution in the presence of potassium ions.

The depolarized dynamic light scattering data are, however, in good agreement with hydrodynamic model calculations for a tetraplex structure that consists of four individual strands, but only 8 bases in length (see Figure 7, 8, and the schematic representation in Figure 2c). This model comes very close to the conformation shown in Figure 2b and suggests that under the given salt conditions the 14-mer d[TTGGGGTTGGGGTT] forms a "hairpin" quadruplex structure in aqueous solution. This conclusion is substantiated by the polarized light scattering experiments as shown in Figure 8. Again, the experimental translation diffusion coefficients are in best agreement with the hydrodynamic predictions for the 8-mer quadruplex structure.

From a comparison of Figures 7 and 8, it becomes obvious that the difference between the translational diffusion coefficients for the various model conformations is less distinctive than for the rotational correlation times (or equivalently rotational diffusion coefficients), making it more difficult to differentiate between the individual conformations from translational motion alone. As discussed above, the reorientation of molecules is more strongly dependent on their size and shape, and Figures 3 and 7 clearly elucidate the higher sensitivity of the depolarized dynamic light scattering experiments.

While in 1.02 and 1.38 mM solutions the translation diffusion coefficient is independent of concentration, we observed a larger D_t for the highest oligonucleotide concentration studied. This effect is probably due to a concentration dependence of the apparent translational diffusion coefficient as measured in polarized dynamic light scattering and has

Table 2: Comparison of Experimental and Calculated Hydrodynamic Properties for the Aptamer d[GGTTGGTGTGGTTGG]

	exptl values		hydrodynamic model calculations		underlying conformations for the model calculations
	D_t^{20} [10^{-6} cm^2/s]	τ_r^{20} [ns]	τ_r^{20} [ns]	D_t^{20} [10^{-6} cm^2/s]	
duplex 16-mer	1.14	11.7	11.8	1.18	Watson−Crick duplex
"hairpin" 17-mer	1.46	4.2	4.28	1.44	Watson−Crick "hairpin"
15-mer	1.80	2.48	1.99	2.57	intramolecular quadruplex
			6.0	1.63	open single strand
			10.67	1.23	intermolecular quadruplex

Table 3: Comparison of Experimental and Calculated Hydrodynamic Properties for Intra- and Intermolecular Quadruplex Structures

	exptl values		model calculations		
sequences	D_t^{20} [10^{-6} cm^2/s]	τ_r^{20} [ns]	τ_r^{20} [ns]	D_t^{20} [10^{-6} cm^2/s]	proposed structure
8-mer, 3.12 mM, 48 mM NaCl [16]	1.34	4.3	4.3	1.34	intermolecular quadruplex
14-mer, 1.38 mM, 45 mM KCl	1.48	4.71	4.3	1.34	dimer "hairpin" intermolecular quadruplex
15-mer, 1.48 mM, 53 mM KCl	1.80	2.48	1.99	2.57	intramolecular quadruplex

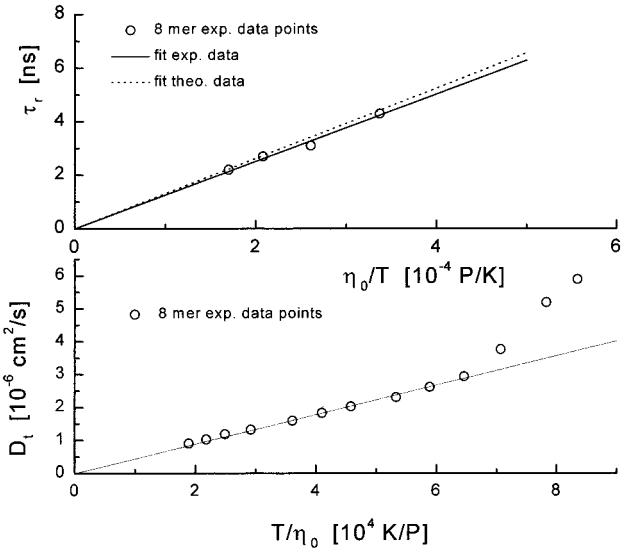

FIGURE 6: Temperature dependence of the rotational relaxation time and translation diffusion coefficient of the 8-mer (○); 3.12 mM in 48 mM NaCl. The deviation from the SE behavior at high temperature indicates a melting of the quadruplex structure.

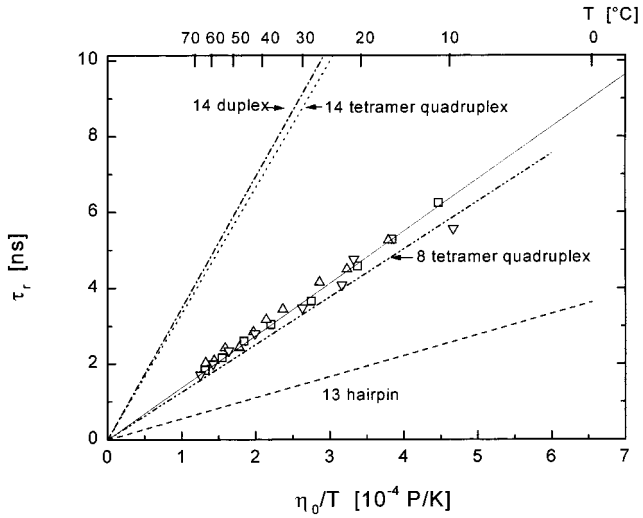

FIGURE 7: Rotation correlation times of the 14-mer d[TTGGGGTTGGGGTT] at different DNA concentrations. The salt concentration varies between 16 mM KCl [(△)1.94 mM DNA] and 45 mM KCl [(□)1.38 mM and (▽)1.02 mM DNA]. Comparison with experimental data from the 8-mer (○), which forms an intermolecular quadruplex structure. Hydrodynamic model calculations for a 14 bp Watson−Crick duplex (- -), a quadruplex structure (•••) composed of four single-strands (14 bases in length; see Figure 1c), and a 13-mer d[CGCGTTGTTCGCG] Watson−Crick "hairpin" structure (identical with experimental data (*19*)).

been observed for other short DNA-fragments in "hairpin" or double-helical conformation (*19*). The rotational diffusion coefficient for the same oligonucleotides is known to be concentration-independent (*19*).

Melting of the quadruplex structures. For all model compounds studied, we observed a deviation of D_t from the Stokes−Einstein equation at high temperature. The translation diffusion coefficients of the 15-mer (Figure 4) and of the 14-mer (Figure 8) fall below the Stokes−Einstein predictions at high temperature, while for the 8-mer, we observed a significant increase of D_t beyond $T \approx 55$ °C. This, for a momentary contradictory effect, can be explained by the different melting behavior of the oligonucleotides. Both, the 15-mer and the 14-mer form compact quadruplex conformations at low temperature in the presence of KCl by intramolecular refolding of the molecules (see Figure 2a and 2 b). Melting leads to more elongated single-stranded structures. Correspondingly, we observe a decrease in D_t due to an increase in the structural anisotropy of the molecules. On the other hand, because quadruplex formation of d[TTGGGGTT]$_4$ occurs by intermolecular interaction, dissociation of the four-stranded 8-mer provides single-strands of smaller size, which is manifested in an increase in the translational diffusion coefficient.

The depolarized component of the scattering intensity is proportional to the square of the optical anisotropy ($\beta = \alpha_{\parallel} - \alpha_{\perp}$) of the particles (*12*), with

$$I_{VH} \sim (\beta^2)N \tag{9}$$

For oligonucleotides, (β) is determined by the relative orientation of the bases within the molecule. Eimer and Dorfmüller (*9*) have observed that the formation of tetramer structures from 5′-GMP is accompanied by a dramatic increase in the depolarized intensity of scattered light, much stronger than observed in I_{VV}. Accordingly, we can assume that the quadruplex structures of the oligonucleotide reveal a much stronger depolarized scattering intensity than the single-stranded conformations of the same molecules. Therefore, in the depolarized light scattering spectra the dynamics of

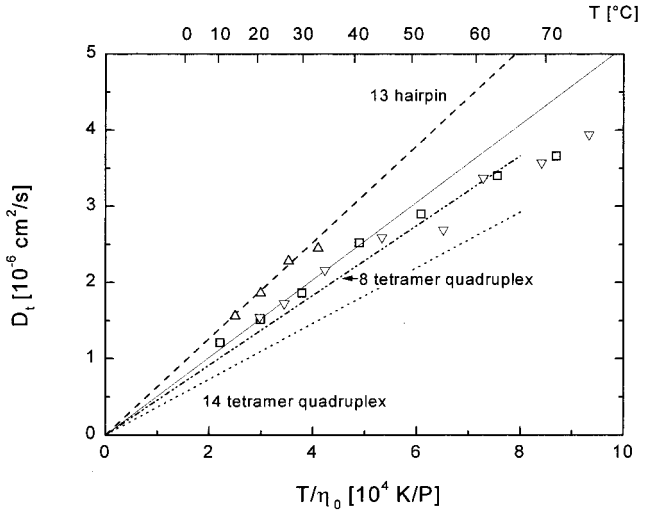

FIGURE 8: Stokes−Einstein plot of the translational diffusion coefficient of the 14-mer at different DNA concentrations. The salt concentration varies between 16 mM KCl [(△)1.94 mM DNA] and 45 mM KCl [(□)1.38 mM and (▽)1.02 mM DNA]. The full line correspond to a linear regression of the experimental data of 1.38 mM and 1.02 mM DNA. Comparison with experimental data from the 8-mer, which forms an intermolecular quadruplex structure. Hydrodynamic model calculations for a quadruplex structure composed of four single-strands (14 nucleobases in length; see Figure 2c), and a 13-mer d[CGCGTTGTTCGCG] Watson−Crick "hairpin" structure.

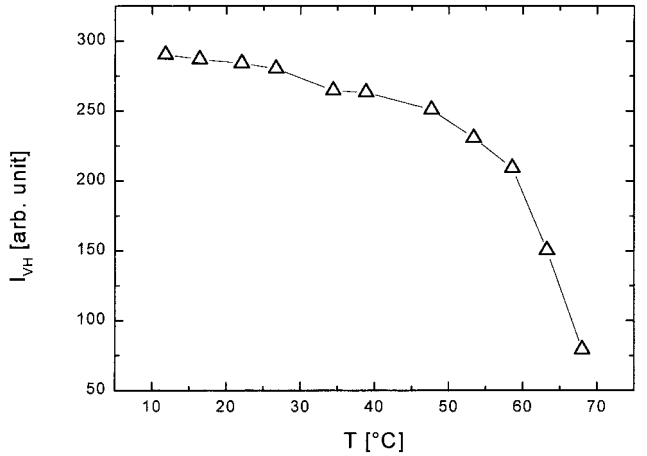

FIGURE 9: Temperature dependence of the depolarized integrated scattering intensity (I_{VH}) of the 14-mer (1.94 mM) in 16 mM KCl.

the melted structures are masked (by the stronger scattering of the quadruplex structures), and hence, the line broadening is still dominated by the reorientational motion of the quadruplex structures. Nevertheless, as shown in Figure 9, melting of these structures can be detected by a decrease of the depolarized light scattering intensity in the spectra.

CONCLUSIONS

The transport properties of molecules, their translational diffusion coefficient, and especially the rotational diffusion coefficient are sensitive parameters to characterize the molecular dimensions, and hence, the conformation of oligonucleotides in solution. For selected G-DNA model compounds, we have demonstrated that a comparison of experimental data from polarized and depolarized dynamic light scattering with hydrodynamic model predictions allows one to distinguish between intra- and intermolecular quadruplex structures. At the same time, the formation of elongated single-stranded or Watson−Crick double-helical B-DNA conformations could be ruled out under the given salt and DNA concentration conditions. Presently, we are investigating the potential of these techniques to characterize equilibrium situations in mixtures of polymorphous G-DNA structures.

Dynamic light scattering has the advantage of being a noninvasive method, providing information about the size and shape of molecules under different environmental conditions in solution. It is feasible to follow conformational transitions that are induced by low molecular weight messenger molecules or ions, changes in ion composition, salt concentration, pH, or solvent composition. DLS, therefore, furnishes valuable complementary information to high-resolution X-ray crystallography and NMR-spectroscopy. In addition, it is a powerful tool to characterize intermolecular interactions, such as DNA−DNA, DNA−RNA, and DNA−protein complexes that are essential for numerous biological processes.

ACKNOWLEDGMENT

The research was sponsored by grants from the Deutsche Forschungsgemeinschaft and the Fond der Chemischen Industrie. We gratefully acknowledge the technical assistance and fruitful discussions with Dr. Christian Borsdorf and Dr. Thomas Hellweg.

REFERENCES

1. Henderson, E., Hardin, C. C., Walk, S. K., Tinoco, I. Jr., and Blackburn, E. H. (1987) *Cell 51*, 899−908.
2. Blackburn, E. H., and Szostak, J. W. (1984) *Annu. Rev. Biochem. 53*, 163−194.
3. Guschlbauer, W., Chantot, J. F., and Thiele, D. (1990) *J. Biomol. Struct. Dyn. 8*, 491−511.
4. Williamson, J. R. (1994) *Annu. Rev. Biophys. Biomol. Struct. 23*, 703−730.
5. Phillips, K., Dauter, Z., Murchie, A. I. H., Lilley, D. M. J., and Luisi, B. (1997) *J. Mol. Biol. 273*, 171−182.
6. Kettani, A., Bouaziz, S., Gorin, A., Zhao, H., Jones, R. A., and Patel, D. J. (1998) *J. Mol. Biol. 282*, 619−636.
7. Blume, S. W., Guarcello, V., Zacharias, W., and Miller, D. M. (1997) *Nucleic Acids Res. 25*, 617−625.
8. Zimmerman, S. B., Cohen, G. H., and Davies, D. R. (1991) *J. Mol. Biol. 92*, 181−192.
9. Eimer, W., and Dorfmüller, T. (1992) *J. Chem. Phys. 96*, 6790−6800.
10. Sen, D., and Gilbert, W. (1992) *Biochemistry 31*, 65−70.
11. Chen, F.-M. (1992) *Biochemistry 31*, 3769−3776.
12. Berne B. J., Pecora, R. (1975) *Dynamic Light Scattering*, John Wiley and sons.
13. Eimer, W., Niermann, M., Eppe, M. A., and Jockusch, B. M. (1993) *J. Mol. Biol. 229*, 146−152.
14. W. Eimer, W., Williamson, J. R., Boxer, S. G., and Pecora, R. (1990) *Biochemistry* 29, 799−811.
15. Garcia de la Torre, J., Navarro, S., and Lopez Martinez, M. C. (1994) *Biophys. J. 66*, 1573−1579.
16. Niermann, M. (1996) Ph.D. Thesis, Bielefeld, Cuvillier Verlag, Göttingen, Germany.
17. van Cittert, P. H. (1931) *Z. Phys. 69*, 298−308.
18. Schmitz, K. S. (1990) in *An Introduction to Dynamic Light Scattering by Macromolecules*, pp 11−28, Academic Press, San Diego, CA.
19. Eimer, W., and Pecora, R. (1991) *J. Chem. Phys. 94*, 2324−2329.
20. Provencher, S. W. (1982) *Comput. Phys. Commun. 27*, 213−239.
21. Harding, S. E. (1995) *Biophys. Chem. 55*, 69−93.
22. Niermann, M., Bolten, M., and Eimer, W. (1999) submitted.

23. Garcia de la Torre, J., and Bloomfield, V. A. (1981) *Q. Rev. Biophys. 14*, 81−139.
24. HyperChem, Molecular Modeling System, Autodesk inc., 1992.
25. Protein Data Bank, Chemistry Department, Building 555, Brookhaven National Laboratory, Upton, NY 11973.
26. van Gunsteren, W. F., and Berendsen, H. J. C. (1986) Groningen molecular simulations (GROMOS) Library manual, University of Groningen, Groningen.
27. Lee, B., and Richards, F. M. (1971) *J. Mol. Biol. 55*, 379−400.
28. Padmanabhan, K., Padmanabhan, K. P., Ferrara, J. D., Sadler, J. E., and Tulinsky, A. (1993) *J. Biol. Chem. 268*, 17651−17654.
29. Macaya, R. F., Schultze, P., Smith, F. W., Roe, J. A., and Feigon, J. (1993) *Proc. Natl. Acad. Sci. 90*, 3745−3749.
30. Marathias, V. M., Wang, K. Y., Kumar, S., Pham, T. Q., Swaminathan, S., and Bolton, P. H. (1996) *J. Mol. Biol. 260*, 378−394.
31. Wang, Y., and Patel, D. J. (1993) *J. Mol. Biol. 234*, 1171−1183.
32. Dote, J. L., and Kivelson, D. (1983) *J. Phys. Chem. 87*, 3889−3895.
33. Balagurumoothy, P., Brahmachari, S. K., Mohanty, D., Bansal, M., and Sasisekharan, V. (1992) *Nucleic Acid Res. 20*, 4061−4067.
34. Williamson, J. R., and Boxer, S. G. (1989) *Biochemistry 28*, 2819−2831.
35. Haber-Pohlmeier, S. (1995) Ph.D. Thesis, Bielefeld, Germany.

BI990750P